Optimal Configuration of Fractional Frequency Reuse System for LTE Cellular Networks

Muhieddin Amer, *Senior Member, IEEE*
Rochester Institute of Technology, Dubai, UAE
mxaeee@rit.edu

***Abstract*—In interference-limited OFDMA systems, fractional frequency reuse (FFR) algorithms can be used to combine the superior performance offerings of a universal reuse plan near cell center and a higher reuse plan near cell edge. A proper configuration of FFR requires knowledge of throughput statistics at all locations in the cell coverage area. This paper introduces an analytical optimization technique to configure a FFR solution for the downlink of LTE cellular system based on a throughput model developed herein. The optimal configuration is based on maximizing the average sector throughput subject to a minimum cell-edge performance and other performance constraints related to the standard reuse plans.**

Keywords – Fractional Frequency Reuse; FFR Optimization; Throughput Modeling; LTE Networks

I. INTRODUCTION

Long Term Evolution (LTE) offers new mechanisms to improve the spectral efficiency at cell edge through H-ARQ, power control with fractional path loss compensation, and interference control using frequency reuse partitioning [1]. Under an interference-limited operation, LTE throughput at cell edge is often unacceptable with a reuse plan of N=1 [2]. Higher reuse plans such as N=3 and N=7 can improve the cell-edge performance, but they reduce the cell-center throughput and often compromise the cell average throughput. As a result, N=7 reuse has not been considered as an effective solution to the cell-edge problem especially for quasi interference-limited networks. Fractional Frequency Reuse (FFR) is a partitioning reuse plan that can be used to balance the link throughput across the coverage area by combining a low-order reuse plan near cell center and a high-order reuse plan near cell edge [3]–[7]. A numerical technique was proposed to configure the FFR algorithm in [6]. An analytical approach is desired for the FFR design and optimization. In addition, the FFR algorithm must meet certain performance conditions and constraints in order to maximize its offering. For example, the throughput realized through FFR must exceed that of a universal reuse 1 at cell edge and that of a reuse 3 near cell center and must exceed a minimum absolute cell-edge throughput. In this case, an optimal configuration of the algorithm requires the throughput statistics at all locations in the cell coverage area. System-level simulations can be used to create SINR-throughput relationships for the different channel models e.g., [8], [9]. Likewise, analytical models for SINR distribution in fast fading channels are available in the literature, e.g., [10]. The models, however, are required to provide explicit relationships among link throughput, system design parameters, and user location and must offer a mechanism to design and optimize a technical feature such as FFR given the large array of system parameters and deployment scenarios. In this paper, analytical models for LTE downlink throughput for different reuse plans are introduced and used to design an optimal configuration of the FFR algorithm. The models adapt accurately to the radio environment and user equipment (UE) location and capture all technology and product performance parameters in simple closed-form formulas.

The remainder of the paper is organized as follows. In section II, models for the downlink SINR and throughput as functions of UE location are developed for N=1 and N=3 reuse plans. An analytical approach is proposed in section III for FFR optimization. Results are presented in section IV, followed by conclusions in section V.

II. SINR and THROUGHPUT MODELS

Consider the two-tier cell layout of Fig. 1 that consists of 57 sectored cells with a uniform cell radius R. The UE is moving between the cell center and cell edge of cell-sector 1α on the 0-degree trajectory as shown in the figure. The received signal-to-interference-plus-noise ratio (SINR) in the downlink of the LTE system at distance r from eNB can be written as

$$\gamma = \left[SIR^{-1} + \left(\frac{PG/L}{\beta n W N_o}\right)^{-1}\right]^{-1}, \quad (1)$$

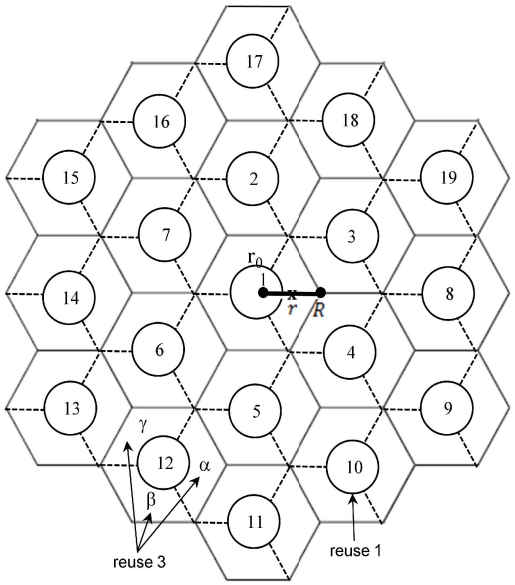

Figure 1. A 57-sector layout with FFR reuse plan. The UE is located at distance r from cell 1, sector α.

978-1-4673-1881-5/12/$31.00 ©2012 IEEE

where P is the total eNB transmit power and G is the antenna gain of the transmit-receive chain less any cable losses, W = 180kHz is the bandwidth of one resource block (RB), n is number of RBs available for data in the LTE bandwidth, and β is the fraction of the bandwidth allocated to the LTE user as permitted by the reuse plan (e.g., β = 1/3 for N=3). $N_o = KTF$ is the thermal noise power spectral density, including the receiver noise figure F. L is the path loss between the transmit and receive antennas. For macrocellular deployment, L follows the widely accepted model [11]

$$L(dB) = A + 10\alpha.log(r) + \chi + \vartheta, \tag{2}$$

where A is the mean path loss at $r = 1km$, α is the propagation exponent, χ represents design losses and margins in decibel, and ϑ is a random variable representing the signal variation due to shadowing.

The signal-to-interference ratio (SIR) in (1) is dependent on the traffic model, reuse plan, and UE geometry with respect to the serving sector and interferers. If all RF signals propagate according to the inverse α–th power law and assuming full traffic buffers on all serving sectors, then the SIR with I co-cells can be written as

$$SIR = \frac{r^{-\alpha}\, 10^{\vartheta_s/10}}{\sum_{i=1}^{I} d_i^{-\alpha}(r)\, 10^{\vartheta_i/10}}, \tag{3}$$

where d_i is the distance between the UE and the i^{th} interferer and ϑ_s and ϑ_i are mutually identical and statistically independent random variables representing the log-normal shadowing on the serving sector and the i^{th} interferer. All shadowing random variables are assumed to have a standard deviation of σ = 8dB.

Table I summarizes the co-cell distances for frequency reuse plans 1 and 3. For reuse 1 (N=1), the average combined inter-cell interference (ICI) contribution from 8β and 8γ arrives at a distance of $R(3 - r/R)$ if the antenna's 3-dB beamwidth is at $\pm 60^0$ from its boresight. For reuse 3 (N=3), the available resource blocks (RB) available in the LTE bandwidth are divided into three equal groups and assigned to sectors α, β, and γ. The allocation of the RB groups to the sectors is done on the basis that the adjacent neighbors of a sector use different RB sets, so dominant tier 1 interferers are eliminated. In this deployment, the UE receives ICI from tier 1 cell-sector 6α and 7α only. From tier 2 cells, the UE receives ICI from 12α, 16α, 13α, 15α, and 14α.

Expressing (3) in decibel and defining $\lambda_i = d_i/R$, we obtain

$$SIR(dB) = -10\alpha log\left(\frac{r}{R}\right) + \vartheta_s - \vartheta_I, \tag{4}$$

where $\vartheta_s = N(0, \sigma^2)$ and

$$\vartheta_I = 10log\left(\sum_{i=1}^{I} \lambda_i^{-\alpha}(r)\, 10^{\vartheta_i/10}\right) \tag{5}$$

is modeled as $N(\mu_I, \sigma_I^2)$. Noting that ICI decays exponentially in r, the model for μ_I in decibel, takes the form

$$\mu_I = 10a\alpha.log\left(\frac{r}{R}\right) + b. \tag{6}$$

TABLE I. CO-CELL DISTANCES BETWEEN UE AT DISTANCE r FROM eNB AND ith INTERFERER

Reuse Plan	Interferers	Normalized co-cell distance $\lambda = d/R$
1	2β, 5γ	$\sqrt{(r/R)^2 + 3}$
1	3β, 4γ	$\sqrt{(r/R)^2 - 3r/R + 3}$
1, 3	6α, 7α	$\sqrt{(r/R)^2 + 3r/R + 3}$
1	9γ, 19β	$\sqrt{(r/R)^2 - 6r/R + 12}$
1	10γ, 18β	$\sqrt{(r/R)^2 - 3r/R + 9}$
1	11γ, 17β	$\sqrt{(r/R)^2 + 12}$
1, 3	12α, 16α	$\sqrt{(r/R)^2 + 3r/R + 9}$
1, 3	13α, 15α	$\sqrt{(r/R)^2 + 6r/R + 12}$
1, 3	14α	$3 + r/R$
1	8β+8γ	$3 - r/R$

The model for μ_I at any distance r must adapt to the propagation exponent α and must be optimized over its practical range. Numerical analysis on ϑ_I for σ = 8dB and α in the range between 3 to 4 reveals that the parameters (a, b) for best MMSE curve fitting are modeled by

$$a_1 = 0.11, \quad a_3 = -0.16, \tag{7}$$

and

$$b_1 = 14.7 - 1.9\alpha,, \quad b_3 = 12.8 - 5\alpha, \tag{8}$$

where the subscripts 1 and 3 refer to reuse plans 1 and 3, respectively. The standard deviation is largely independent of distance for both reuse scenarios with

$$\sigma_{I,1} = 4\text{dB}, \quad \sigma_{I,3} = 4.5\text{dB}. \tag{9}$$

Using (5) in (3), it is straightforward to show that the average SIR including shadowing variations on all signals is given by

$$\overline{SIR}\,(dB) = -10\alpha\log\left(\frac{r}{R}\right) - \mu_I + \frac{ln10}{10}(\sigma_s^2 + \sigma_I^2)/2. \tag{10}$$

Using (2) and (4) in (1) and using the decibel values for P, G, and N_o, the SINR can be written as

$$\gamma = 10^{\vartheta_s/10}\left(10^{\vartheta_I/10}\left(\frac{r}{R}\right)^{\alpha} + \beta nW \cdot 10^{-\frac{P+G-N_O-A-\chi}{10}} r^{\alpha}\right)^{-1}. \tag{11}$$

The LTE link throughput can be computed using Shannon formula. However, Shannon formula is based on AWGN channel assumption with infinite code block size. Actual link throughput is reduced by several implementation issues in addition to loss due to overhead reserved for control channels and reference symbols. Therefore, the link throughput is adjusted with correction factors to bring it in line with practical system deployment. The average link throughput normalized to nW (i.e., the spectral efficiency) can be written as

$$T = \beta\eta_T.E\left[log_2(1 + \eta_\gamma\gamma)\right], \tag{12}$$

where η_γ the SINR efficiency factor that accounts for losses due to limited block code length and performance limitations of practical receiver algorithms. The throughput efficiency factor η_T accounts for losses due to limited MCS granularity, practical filter designs, overhead for cyclic prefix, reference symbols, and common control channels. For a SISO LTE baseline system in a typical urban (TU) channel, the best-fit to system-level simulations over the practical SINR range yields $\eta_\gamma = 0.5$ and $\eta_T = 0.56$ [12]. The reference showed that the deviation of the spectral efficiency computed from the modified Shannon formula is within 5% from simulation.

The average throughput can be approximated using Jensen's inequality. Noting that T is concave in γ, the average link throughput is upper bounded by

$$T = \beta\eta_C \cdot \begin{cases} log_2[1+\eta_\gamma\bar{\gamma}], & \bar{\gamma} \le \gamma_0 \\ log_2[1+\eta_\gamma\gamma_0], & \bar{\gamma} > \gamma_0 \end{cases}, \tag{13}$$

where, for interference-limited systems, $\bar{\gamma}$ is given by (10). In general, $\bar{\gamma}$ can be approximated by

$$\bar{\gamma} = E\left[10^{\vartheta_S/10}\right]\left(E\left[10^{\vartheta_I/10}\right]\left(\frac{r}{R}\right)^{\alpha} + \beta nW \cdot 10^{-\frac{P+G-N_O-A-\chi}{10}} r^{\alpha}\right)^{-1}$$
$$= 10^{\frac{ln10}{2}\left(\frac{\sigma_S}{10}\right)^2}\left(10^{\frac{b}{10}} 10^{\frac{ln10}{2}\left(\frac{\sigma_I}{10}\right)^2}\left(\frac{r}{R}\right)^{(1+a)\alpha} + \beta nW \cdot 10^{-\frac{P+G-N_O-A-\chi}{10}} r^{\alpha}\right)^{-1} \tag{14}$$

The link throughput is limited by the 64QAM 5/6 MCS allowed by LTE in the downlink. Therefore, throughput saturates as γ exceeds γ_0. Again, for a SISO LTE system in a TU channel, γ_0 is typically in the order of 27dB for low to moderate mobile speeds based on system simulation and field trial [12], [13].

The model created above for SINR makes it possible to develop assessment for LTE link throughput as a function of distance. The model captures all parameters related to product, technology, radio environment, and cell geometry in a simple formula and offers a practical simplification to the throughput performance. Of a particular interest is the link throughput at cell edge, which can readily be assessed for different ISDs, link budgets, bandwidths, and reuse plans. The latter is manifested in the model through the different settings of (a, b). An appreciation of the efficacy of the model is merited through its use in the design and optimization of technical features such as FFR as discussed next.

III. FFR Optimization

Equation (10) indicates that the average improvement in SIR with N=3 reuse is $b_1 - b_3 + \frac{ln10}{10}(\sigma_{I,3}^2 - \sigma_{I,1}^2)/2$ decibels compared with the universal reuse plan. For $\alpha = 3.76$, the improvement reaches 13.9dB at cell edge. In an interference-limited scenario, (13) indicates that N=3 system can outperform N=1 at cell edge using only 15% of its spectrum. Since N=1 outperforms N=3 near cell center, this example demonstrates that the throughput performance can be improved if the two reuse plans are combined using a hybrid partitioning reuse system. This leads to a Fractional Frequency Reuse system that consists of two reuse plans. An example of a FFR system is depicted in Fig.1 where the available resource blocks are divided into two groups. Group one with a fraction f_1 of the total resource blocks is allocated to N=1 users. This is deployed within a distance r_0 from the cell center. The remaining resource blocks are allocated to N=3 users and subdivided into three groups and each sector receives $(1-f_1)/3$ of the resource blocks. Under this configuration, each sector can transmit on $(1+2f_1)n/3$ of the resource blocks and the resource utilization varies between 33% and 100%. The model developed above can be used to find the optimum allocation of bandwidth between the two reuse plans and the optimum boundary where switching from N=1 to N=3 should occur.

The cell-edge performance can be further improved in coverage-limited scenarios by allocating more power to N=3 resource blocks. Denote by ξ the power ratio of reuse 3 to reuse 1 resource blocks, the average SINRs associated with the two reuses making the FFR plan are given by

$$\gamma_1 = 10^{\frac{ln10}{2}\left(\frac{\sigma_S}{10}\right)^2}\left(10^{\frac{b_1}{10}} 10^{\frac{ln10}{2}\left(\frac{\sigma_{I,1}}{10}\right)^2}\left(\frac{r}{R}\right)^{(1+a_1)\alpha} + nW \cdot \left(f_1 + \frac{\xi(1-f_1)}{3}\right) \cdot 10^{-\frac{P+G-N_O-A-\chi}{10}} r^{\alpha}\right)^{-1}, \quad r \le r_0 \tag{15a}$$

$$\gamma_3 = 10^{\frac{ln10}{2}\left(\frac{\sigma_S}{10}\right)^2}\left(10^{\frac{b_3}{10}} 10^{\frac{ln10}{2}\left(\frac{\sigma_{I,3}}{10}\right)^2}\left(\frac{r}{R}\right)^{(1+a_3)\alpha} + nW \cdot \left(\frac{f_1}{\xi} + \frac{1-f_1}{3}\right) \cdot 10^{-\frac{P+G-N_O-A-\chi}{10}} r^{\alpha}\right)^{-1}, \quad r_0 < r \le R. \tag{15b}$$

The FFR spectral efficiency as a function of distance can now be written as

$$T_{FFR} = \eta_C \begin{cases} f_1 \begin{cases} log_2[1+\eta_\gamma\gamma_0], & \gamma_1 > \gamma_0 \\ log_2[1+\eta_\gamma\gamma_1], & r \le r_0 \end{cases} \\ \frac{1-f_1}{3} \begin{cases} log_2[1+\eta_\gamma\gamma_0], & \gamma_3 > \gamma_0 \\ log_2[1+\eta_\gamma\gamma_3], & r_0 \le r \le R \end{cases} \end{cases} \tag{16}$$

A proper configuration of the FFR algorithm requires the solution to satisfy certain performance conditions. In particular, the FFR throughput must exceed the standard N=3 throughput near cell center and must exceed the universal N=1 throughput at cell edge. Since $\gamma > \gamma_0$ near cell center, the first condition yields

$$f_{1,min} = \frac{1}{3}. \tag{17}$$

The second condition yields $f_{1,max}$ and can be written as

$$\frac{1-f_1}{3} \cdot log_2\left[1+\eta_\gamma 10^{\frac{ln10}{2}\left(\frac{\sigma_S}{10}\right)^2}\left(10^{\frac{b_3}{10}} 10^{\frac{ln10}{2}\left(\frac{\sigma_{I,3}}{10}\right)^2} + nW \cdot \left(\frac{f_1}{\xi} + \frac{1-f_1}{3}\right) \cdot 10^{-\frac{P+G-N_O-A-\chi}{10}} R^{\alpha}\right)^{-1}\right] > log_2\left[1+\eta_\gamma 10^{\frac{ln10}{2}\left(\frac{\sigma_S}{10}\right)^2}\left(10^{\frac{b_1}{10}} 10^{\frac{ln10}{2}\left(\frac{\sigma_{I,1}}{10}\right)^2} + nW \cdot 10^{-\frac{P+G-N_O-A-\chi}{10}} R^{\alpha}\right)^{-1}\right]. \tag{18}$$

Different maximization criteria can be employed to find the optimum settings of f_1 and r_0. However, maximizing the sector average throughput while constraining the cell-edge throughput to a minimum performance and satisfying the conditions in (17) and (18) provides a comprehensive optimization approach and allows for the concurrent

optimization of f_1 and r_0. If the UEs are uniformly distributed over the coverage area, then the optimization problem can be stated as follows

$$\max_{f_1, r_0} \int_{\epsilon}^{r_0} T_{FFR}(r;\, r_0, f_1)dA + \int_{r_0}^{R} T_{FFR}(r;\, r_0, f_1)dA \qquad (19)$$

$$subject\ to \qquad T_{FFR}(R; f_1) = T_0 \qquad (20)$$

$$and \qquad f_{1,min} \le f_1 \le f_{1,max}, \qquad (21)$$

where T_0 is the desired cell-edge throughput. The cell-edge constraint in (20) can be written as

$$\frac{1-f_1}{3}\eta_C . log_2\left[1 + \eta_\gamma 10^{\frac{ln10}{2}\left(\frac{\sigma_s}{10}\right)^2}\left(10^{\frac{b_3}{10}} 10^{\frac{ln10}{2}\left(\frac{\sigma_{I,3}}{10}\right)^2} + nW \cdot \left(\frac{f_1}{\xi} + \frac{1-f_1}{3}\right) \cdot 10^{-\frac{P+G-N_0-A-\chi}{10}} R^\alpha\right)^{-1}\right] = T_0. \qquad (22)$$

Since the cell-edge constraint is independent of r_0, the above optimization problem is reduced to maximizing the average cell throughput with respect to r_0 with f_1 being the solution to the cell-edge constraint in (20) and satisfying $f_{1,min} \le f_1 \le f_{1,max}$. Therefore, the maximization in (19) yields the following solution for $r_{0,opt}$

$$1 + \eta_\gamma 10^{\frac{ln10}{2}\left(\frac{\sigma_s}{10}\right)^2}\left(10^{\frac{b_1}{10}} 10^{\frac{ln10}{2}\left(\frac{\sigma_{I,1}}{10}\right)^2}\left(\frac{r_{0,opt}}{R}\right)^{(1+a_1)\alpha} + nW \cdot \left(f_1 + \frac{\xi(1-f_1)}{3}\right) \cdot 10^{-\frac{P+G-N_0-A-\chi}{10}} r_{0,opt}^\alpha\right)^{-1} = \left[1 + \eta_\gamma 10^{\frac{ln10}{2}\left(\frac{\sigma_s}{10}\right)^2}\left(10^{\frac{b_3}{10}} 10^{\frac{ln10}{2}\left(\frac{\sigma_{I,3}}{10}\right)^2}\left(\frac{r_{0,opt}}{R}\right)^{(1+a_3)\alpha} + nW \cdot \left(\frac{f_1}{\xi} + \frac{1-f_1}{3}\right) \cdot 10^{-\frac{P+G-N_0-A-\chi}{10}} r_{0,opt}^\alpha\right)^{-1}\right]^{\frac{1-f_1}{3f_1}}. \qquad (23)$$

Noting that the throughputs associated with both reuse plans are monotonically decreasing functions in r, (23) indicates that the optimum switching point that maximizes the average sector throughput, if exists, is where the two throughput functions intersect. The solution to (23) may not exist if f_1 is inadvertently set too low to warrant a cell-edge performance significantly above the universal N=1 reuse plan. In this case, the system performs better with N=3. However, when f_1 is subjected to the conditions in (17) and (18), then a unique solution exists.

IV. Results and Discussion

A subset of the simulation parameters used to assess the LTE performance relative to HSPA Release 6 is chosen for this study [1]. A summary of the evaluation parameters is given in Table II. The evaluation methodology assumes a 10MHz macrocellular LTE network with an inter-site distance of 500m. This ISD case represents a heavily interference-limited deployment that gives rise to the lower limit on distance where N=3 outperforms N=1. The path loss model is chosen for a 2GHz system with 20dB building penetration loss and 5dB for other losses. The terminal noise figure is 9dB.

Fig. 2 gives as a function of distance the throughput ratio of reuse 3 with a fractional bandwidth of $(f_1 - 1)/3$ to reuse 1 with a fractional bandwidth of f_1. The figure shows that reuse 3 outperforms reuse 1 at the cell edge with as low as 10% of the spectrum (70% of the spectrum is allocated to reuse 1 users). At $r = R/2$, reuse 3 outperforms reuse 1 using nearly 20% of the spectrum. These results illustrate that there exists a tradeoff between f_1 and r_0 where reuse 1 and 3 can alternate in performance superiority. FFR can combine the better offering of the two reuse plans in an optimal way according to the optimization criteria in (19) – (21).

TABLE II. Evaluation Parameters

Parameter	Value
f_c	2GHz
P	46dBm
B	10MHz
n	50
G	17dBi
N_0F	-165dBm/Hz
A	128.1dB[1]
α	3.76
χ	25 dB
σ	8dB
ξ	0dB
η_γ	0.5
η_C	0.56
γ_0	27dB
ϵ	35m
ISD	500m

[1] Distance in path loss model is in km.

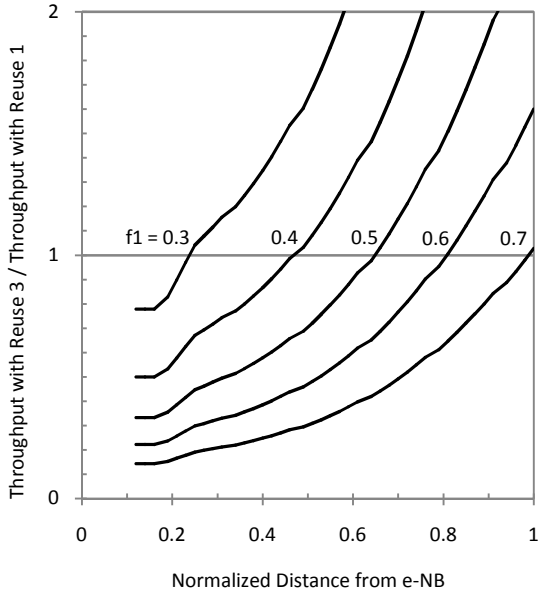

Figure. 2. Ratio of reuse 3 throughput with fractional bandwidth $(f_1 - 1)/3$ to reuse 1 throughput with fractional bandwidth f_1.

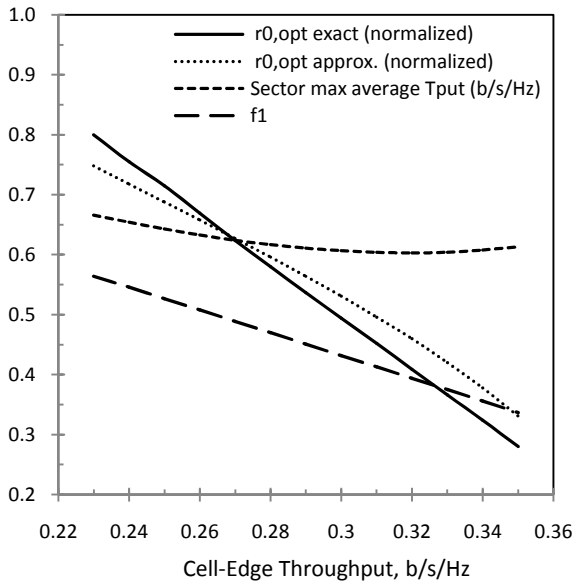

Figure 3. Optimal configuration of FFR.

The relationships between f_1 and $r_{0,opt}$ and the desired cell-edge throughput (T_0) is shown in Fig. 3. The graph is shown for the range of f_1 where FFR can provide benefits over N=1 and N=3 as bounded by the constraints in (17) and (18). The provisioning of the minimum value on f_1 (in order to guarantee that the FFR throughput doesn't fall below N=3 near cell center) sets a lower limit on $r_{0,opt}$. This limit is around 30% of the cell radius. Conversely, the provisioning of the maximum value on f_1 (in order to guarantee that the FFR throughput doesn't fall below N=1 at cell edge) sets an upper limit on $r_{0,opt}$. This limit is around 80% of the cell radius. If the cell-edge throughput is desired to be 0.27 b/s/Hz, then the resource blocks must be allocated equally between the two reuse plans and the optimum switching must occur at 62% of the cell radius. The figure shows that the relationship between $r_{0,opt}$ and T_0 follows a "waterfall" trend. As the requirement on cell-edge throughput increases, f_1 must decrease and the maximization of the sector average throughput requires r_0 to drop rapidly. This indicates that although FFR throughput has a small margin of being above that of N=1 at cell edge, r_0 exhibits a large optimization range. In addition, since the sector average throughput is not very sensitive to cell-edge throughput target, $r_{0,opt}$ can be chosen to be below the value that satisfies a minimum cell-edge throughput. This provides FFR with a performance margin against measurement errors and channel variation.

Practical systems make use of the average SINR measurements reported by the UE to determine if a user at distance r from eNB should be on reuse plan 1 or 3. The SINR can be computed from (15a) at $r = r_{0,opt}$. For example, for $\frac{r_{0,opt}}{R} = 0.62$ ($T_0 = 0.27$ b/s/Hz), switching occurs when γ_1 falls below 6.4dB.

IV. Conclusions

An analytical model for the LTE downlink throughput was proposed and used to optimize the FFR algorithm. The model expresses throughput as a function of distance and captures all system design parameters in a single formula, giving rise to numerous applications in capacity planning and feature optimization of LTE networks. The optimal configuration of the FFR algorithm is based on maximizing the average sector throughput subject to a minimum cell-edge performance and other performance constraints related to reuse 1 and 3. Based on this criterion, it was shown that the FFR algorithm possesses a good optimization range while satisfying all performance constrains. The optimum normalized switching distance decreases from 0.8 to 0.3 and the spectrum allocation to reuse 1 decreases from 57 to 33% as the target cell-edge spectral efficiency increases from 0.23 to 0.35 b/s/Hz. The results indicate that the relationship between the optimum distance and the cell-edge throughput follows a waterfall trend. The maximum sector average throughput is not sensitive to cell-edge throughput, hence allowing network designers to configure the FFR algorithm for higher cell-edge performance targets with a graceful degradation to the average throughput. This drives f_1 and r_0 towards their lower optimization range.

References

[1] 3GPP RAN WG1 Technical Report 25.814 v7.1.0, Physical Layer Aspects for Evolved UTRA, Rel. 7, v7.1.0, Sept. 2006.

[2] B. Ramamurthi, "Cutting edge at the cell edge: Co-channel interference mitigation in emerging broadband wireless systems," *1st International Communication Systems and Networks and Workshops (COMSNETS),* pp. 1-7, Jan. 2009.

[3] R. Rizwan and R. Knopp, "Fractional frequency reuse and interference suppression for OFDMA networks," in *Proc. of the 8th International Symposium on Modeling and Optimization in Mobile, Ad Hoc and Wireless Networks (WiOpt),* pp.273-277, May 2010.

[4] S. W. Halpern, "Reuse partitioning in cellular systems," in *Proc. IEEE 33rd Vehicular Technology Conference*, May 1983, vol. 3, pp. 322–327.

[5] Z. Xie, and B. Walke,, "Frequency reuse techniques for attaining both coverage and high spectral efficiency in OFDMA cellular systems," *IEEE Wireless Comm. & Networking Conf. (WCNC),* pp.1-6, April 2010.

[6] M. Assaad, "Optimal fractional frequency reuse (FFR) in multicellular OFDMA system," in *Proc., IEEE 68th Veh. Technology Conf.*, pp.1-5, Sept. 2008.

[7] Farooq Khan, *LTE for 4G Mobile Broadband - Air Interface Technologies and Performance*, Ambridge University Press, 2009.

[8] S. Wang; J. Wang; J. Xu; Y. Teng, and K. Horneman, "Cooperative component carrier (re-) selection for LTE-Advanced Femtocells," in *Proc. IEEE Wireless Communications and Networking Conference (WCNC),* pp.629-634, March 2011.

[9] A. Farajidana, W. Chen, A. Damnjanovic, T. Yoo, D. Malladi, and C. Lott, "3GPP LTE downlink system performance," *Global Telecommunications Conference (GLOBECOM),* Nov. 2009.

[10] Z. Lin, P. Xiao, and B. Vucetic, "SINR distribution for LTE downlink multiuser MIMO systems," in *Proc. ICASSP*, April 2009, pp. 2833–2836.

[11] T.S. Rappaport, "Wireless Communications: Principles and Practice", Prentice Hall, 2002, Ch. 4.

[12] P. Mogensen, W. Na, I. Kovacs, F. Frederiksen, A. Pokhariyal, K. Pedersen, T. Kolding, K. Hugl, and M. Kuusela, "LTE capacity compared to the Shannon bound," in *Proc. IEEE Vehicular Technology Conference (VTC)*, pp. 1234–1238, April 2007.

[13] R. Irmer et al, "Multisite field trial for LTE and advanced concepts," *IEEE Communications Magazine*, vol. 47, no. 2, pp. 92–98, Feb. 2009.